Supporting Information

Tables [Ia], [Ib], [Ic], [Id]: Major cleavage fragments detected in MALDI-TOF mass experiments for CLB-HyM-10 versus U4A-L4T, CLB-HyM-10 versus XU4A-XL4T, CLB-HyQ-10 versus U4A-L4T, CLB-HyQ-10 versus XU4A-XL4T, respectively. The sequence of the cleavage fragments are arranged in order of decreasing mass peak intensity.

5'-T$_1$- A$_2$- G$_3$ - G$_4$ - A$_5$- G$_6$- A$_7$- A$_8$ - A$_9$- A$_{10}$-T$_{11}$-A$_{12}$-C$_{13}$-3'
3'-A$_{26}$-T$_{25}$-C$_{24}$-C$_{23}$-T$_{22}$-C$_{21}$-T$_{20}$-T$_{19}$-T$_{18}$- T$_{17}$-A$_{16}$-T$_{15}$-G$_{14}$-5'

Duplex U4A-L4T

5'-A$_1$- A$_2$- G$_3$ - G$_4$ - A$_5$- G$_6$- A$_7$- A$_8$ - A$_9$- A$_{10}$-T$_{11}$-A$_{12}$-C$_{13}$-3
3'-T$_{26}$-T$_{25}$-C$_{24}$- C$_{23}$- T$_{22}$-C$_{21}$-T$_{20}$-T$_{19}$-T$_{18}$-T$_{17}$-A$_{16}$-T$_{15}$-G$_{14}$-5'

Duplex XU4A-XL4T

Figure [I]. Autoradiographs showing cleavage of 158-mer (left panels) and 135-mer (right panels) of pBR322 DNA fragment induced by DNase I (footprinting) in the presence of peptide HyQ-10 (upper panels), or induced by incubating with conjugate CLB-HyQ-10 in 5 mM sodium cacodylate buffer (pH 6.5) at 37°C for 30 min (lower panels).

Figure [II]. CD spectra: Panel A: Titration of duplex U4A-L4T versus peptide HyQ-10 at peptide concentrations of 0.5, 1.0, 2.2, 2.4, 2.6, 2.8, 3.0, 3.2, 3.4, 4.0, 5.0, 7.0 μM at 37ºC. Panel B: Corresponding CD difference spectra with the contribution of free duplex and peptide HyQ-10 subtracted. Panel C: Titration of U4A-L4T versus conjugate CLB-HyQ-10 at conjugate concentrations of 0.5, 1.0, 1.5, 1.8, 2.1, 2.2, 2.3, 2.4, 2.5, 2.6, 2.7, 2.8, 3.0, 3.5, 4.0, 5.0 μM at 37ºC. Panel D: Corresponding difference spectra with the contribution of free duplex and conjugate CLB-HyQ-10 subtracted.

Figure [III]. Plots of relative intensity of MALDI-TOF mass peaks of major cleavage fragments induced by conjugates CLB-HyM-10, (panel A) and CLB-HyQ-10 (panel B) on the oligonucleotide duplex U4A-L4T; and plots of relative intensity of MALDI-TOF mass peaks of major cleavage fragments induced by conjugates

CLB-HyM-10 (panel C), and CLB-HyQ-10 (panel D) on the oligonucleotide duplex XU4A-XL4T. Representative MALDI-TOF mass peaks of major cleavage fragments induced by conjugate CLB-HyM-10, (panel E); and conjugate CLB-HyQ-10, (panel F) on the oligonucleotide duplex XU4A-XL4T

Figure [IV]. Proposed DNA cleavage mechanism via depurination and carboxonium ion intermediates induced by CLB-peptide conjugates.

Table [1a]. CLB-HyM-10 versus U4A-L4T

Mass	**Strand**	**Cleavage fragments**	**Proposed cleavage mechanism**
2033.9	Lower	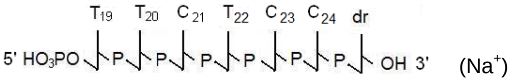	Depyrimidination of T_{18} and T_{25}
2337.3	Upper	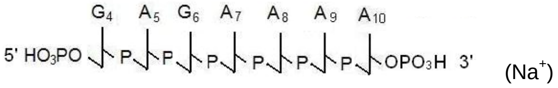	Depurination of G_3 and depyrimidination of T_{11}
2643.2	Upper	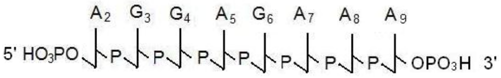	Depyrimidination of T_1 and depurination of A_{10}
1732.3	Upper	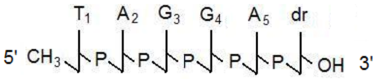	Depurination of G_6
1597.9	Lower	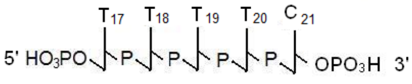	Depurination of A_{16} and depyrimidination of T_{22}
998.3	Lower	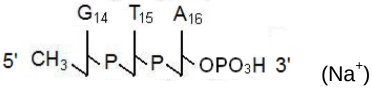	Depyrimidination of T_{17}
2943.8	Lower	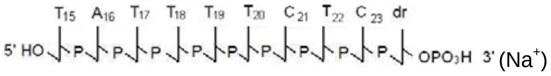	Depurination of G_{14} and depyrimidination of C_{24}
806.3	Upper	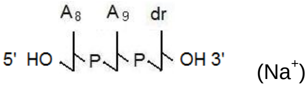	Depurination of A_{10} and A_7
1442.2	Upper	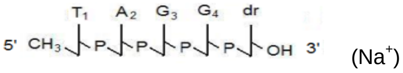	Depurination of A_5
1948.7	Lower	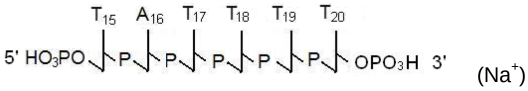	Depurination of G_{14} and C_{21}

Table [Ib]. CLB-HyM-10 versus XU4A-XL4T

Mass	**Strand**	**Cleavage fragments**	**Proposed cleavage mechanism**
998.6	Lower	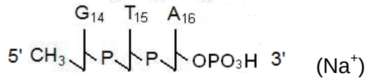	Depyrimidination of T_{17}
1948.5	Lower	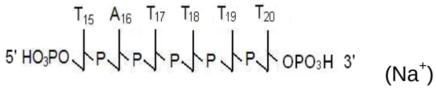	Depurination of G_{14} and depyrimidination of C_{21}
1597.9	Lower	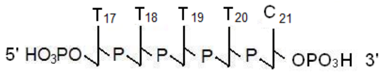	Depurination of A_{16} and depyrimidination of T_{22}
1960.3	Upper		Depyrimidination of C_{13} and depurination of G_6
711.0	Upper	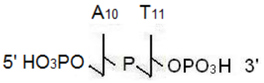	Depurination of A_9 and A_{12}
926.3	Lower	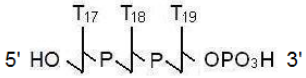	Depurination of A_{16} and depyrimidination of T_{20}
806.1	Upper	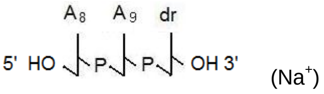	Depurination of A_{10} and A_7
2025.2	Upper	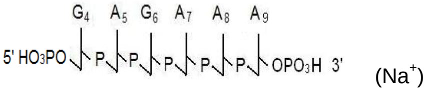	Depurination of G_3 and A_{10}
2033.1	Lower	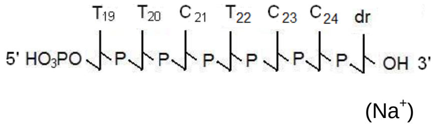	Depyrimidination of T_{18} and T_{25}
2186.9	Upper	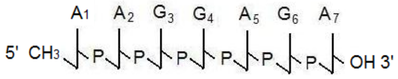	Depurination of A_8

Table [Ic]. CLB-HyQ-10 versus U4A-L4T

Mass	Strand	Cleavage fragments	Proposed cleavage mechanism
712.4	Upper	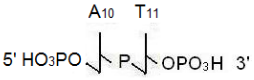	Depurination of A_9 and A_{12}
998.3	Lower	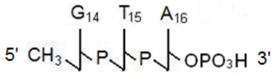 (Na$^+$)	Depyrimidination of T_{17}
1732.7	Upper	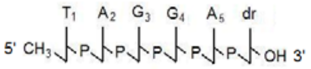	Depurination of G_6
2337.5	Upper	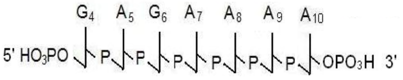 (Na$^+$)	Depurination of G_3 and depyrimidination of T_{11}
2033.9	Lower	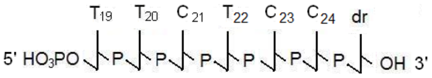 (Na$^+$)	Depyrimidination of T_{18} and T_{25}
2642.6	Upper	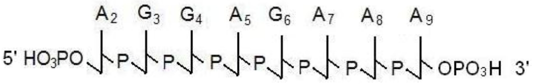	Depyrimidination of T_1 and depurination of A_{10}
1442.3	Upper	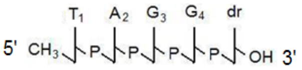 (Na$^+$)	Depurination of A_5
2177.6	Upper	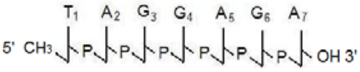	Depurination of A_8
2943.9	Lower	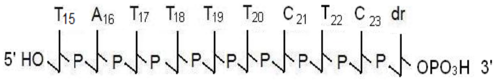 (Na$^+$)	Depurination of G_{14} and depyrimidination of C_{24}
970.7	Upper	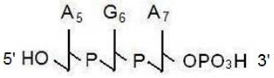	Depurination of G_4 and A_8
926.7	Lower	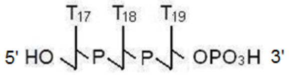	Depurination of A_{16} and depyrimidination of T_{20}
1140.8	Upper	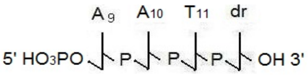	Depurination of A_{12} and A_8
1948.6	Lower	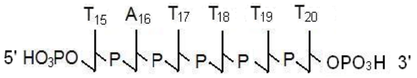 (Na$^+$)	Depurination of G_{14} and depyrimidination of C_{21}

Table [Id]. CLB-HyQ-10 versus XU4A-XL4T

Mass	**Strand**	**Cleavage fragments**	**Proposed cleavage mechanism**
712.7	Upper	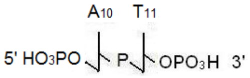	Depurination of A_9 and A_{12}
998.3	Lower	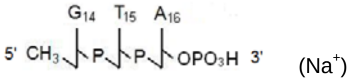	Depyrimidination of T_{17}
2024.8	Upper	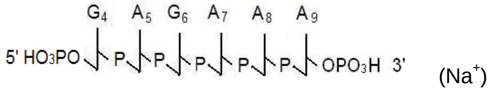	Depurination of G_3 and A_{10}
2033.9	lower	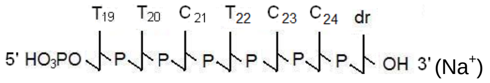	Depyrimidination of T_{18} and T_{25}
970.7	Upper	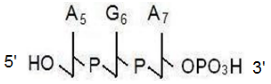	Depurination of G_4 and A_8
1948.7	Lower	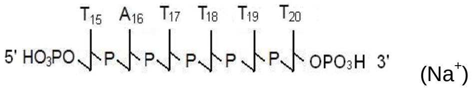	Depurination of G_{14} and depyrimidination of C_{21}
1451.2	Upper	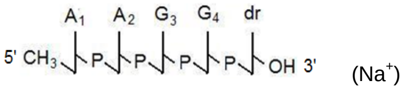	Depurination of A_5
2186.6	Upper	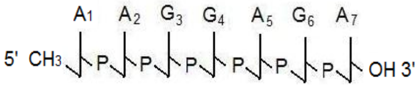	Depurination of A_8

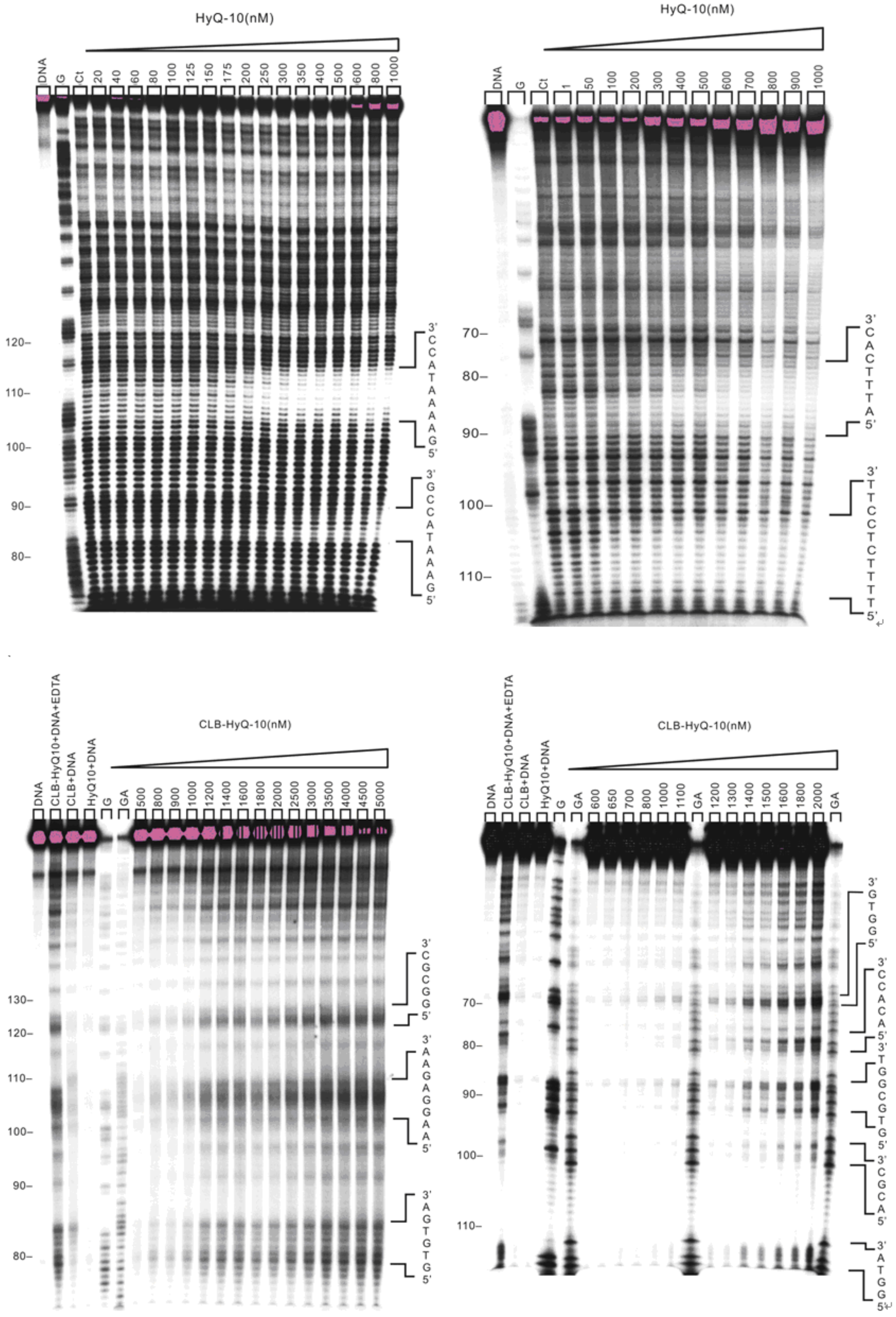
HyQ-10(nM)
DNA
G
Ct
20
40
60
80
100
125
150
175
200
250
300
350
400
500
600
800
1000
120–
110–
100–
90–
80–
3' C C A T A A A A G 5'
3' G C C A T A A A G 5'
HyQ-10(nM)
DNA
G
Ct
1
50
100
200
300
400
500
600
700
800
900
1000
70–
80–
90–
100–
110–
3' C A C T T T A 5'
3' T T C C T C T T T T 5'
CLB-HyQ-10(nM)
DNA
CLB-HyQ10+DNA+EDTA
CLB+DNA
HyQ10+DNA
G
GA
500
800
900
1000
1200
1400
1600
1800
2000
2500
3000
3500
4000
4500
5000
130–
120–
110–
100–
90–
80–
3' C G C G G G 5'
3' A A G A G G A A 5'
3' A G T G T G 5'
CLB-HyQ-10(nM)
DNA
CLB-HyQ10+DNA+EDTA
CLB+DNA
HyQ10+DNA
G
GA
600
650
700
800
1000
1100
GA
1200
1300
1400
1500
1600
1800
2000
GA
70–
80–
90–
100–
110–
3' G T G G 5'
3' C C A C A 5'
3' T G G C G T G 5'
3' C G C A 5'
3' A T G G 5'

Figure [I]

A HyQ-10 / U4A-L4T

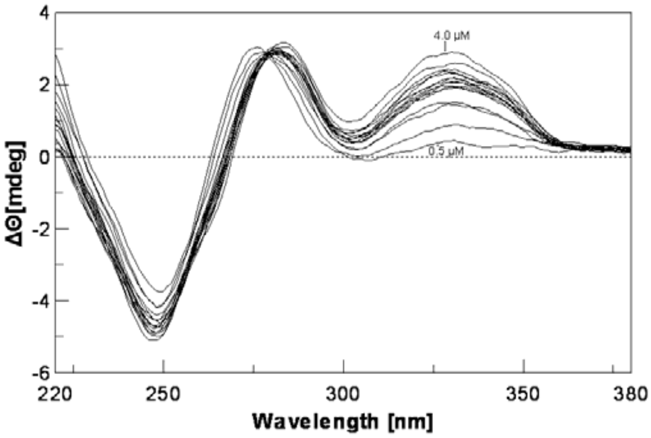

B HyQ-10 / U4A-L4T Difference spectra

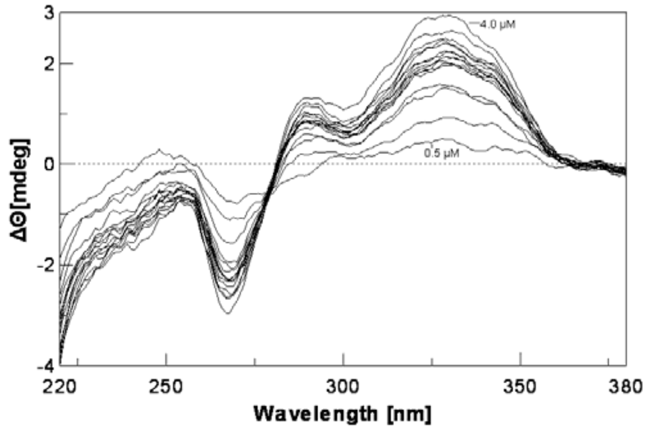

C CLB-HyQ-10 / U4A-L4T

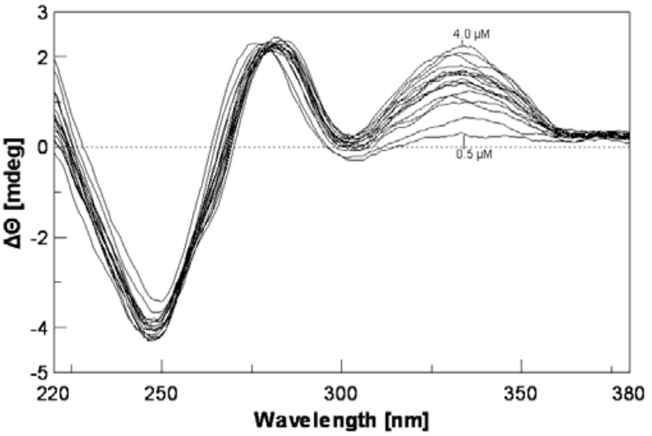

Figure [II]

D CLB-HyQ-10 / U4A-L4T Difference spectra

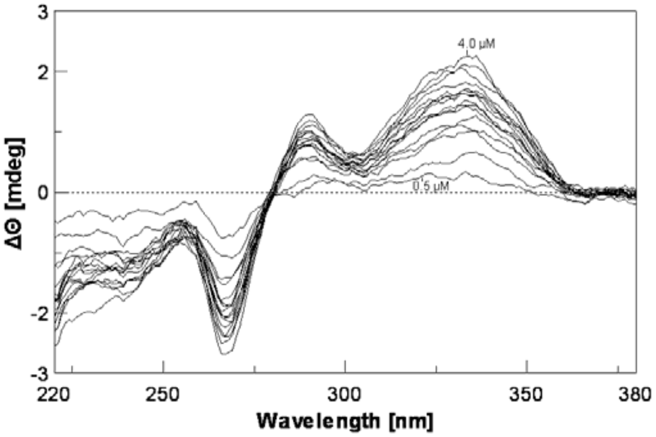

Figure [II]

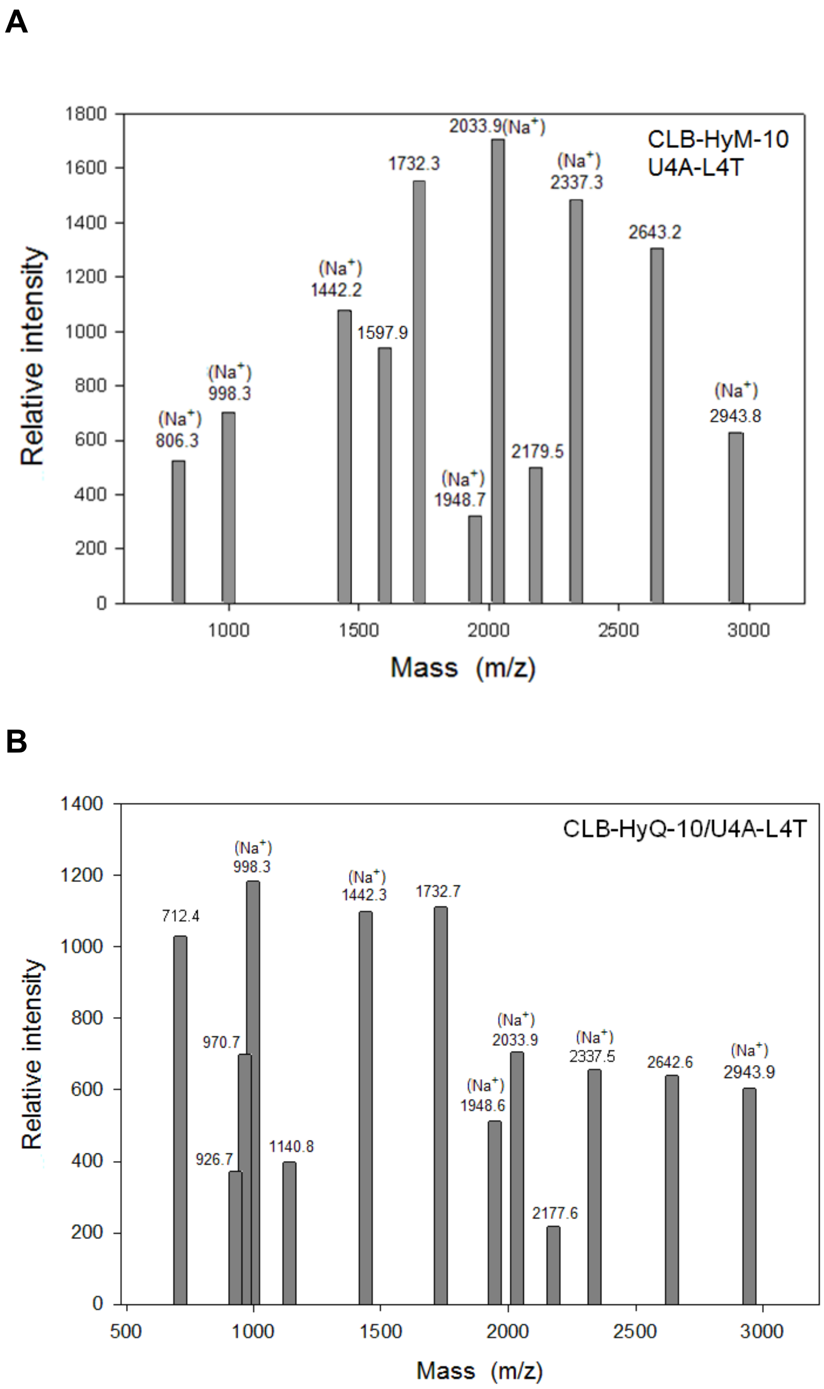
A
CLB-HyM-10
U4A-L4T
Relative intensity
Mass (m/z)
0
200
400
600
800
1000
1200
1400
1600
1800
1000
1500
2000
2500
3000
(Na+) 806.3
(Na+) 998.3
(Na+) 1442.2
1597.9
1732.3
(Na+) 1948.7
2033.9(Na+)
2179.5
(Na+) 2337.3
2643.2
(Na+) 2943.8
B
CLB-HyQ-10/U4A-L4T
Relative intensity
Mass (m/z)
0
200
400
600
800
1000
1200
1400
500
1000
1500
2000
2500
3000
712.4
926.7
970.7
(Na+) 998.3
1140.8
(Na+) 1442.3
1732.7
(Na+) 1948.6
(Na+) 2033.9
2177.6
(Na+) 2337.5
2642.6
(Na+) 2943.9

Figure [III]

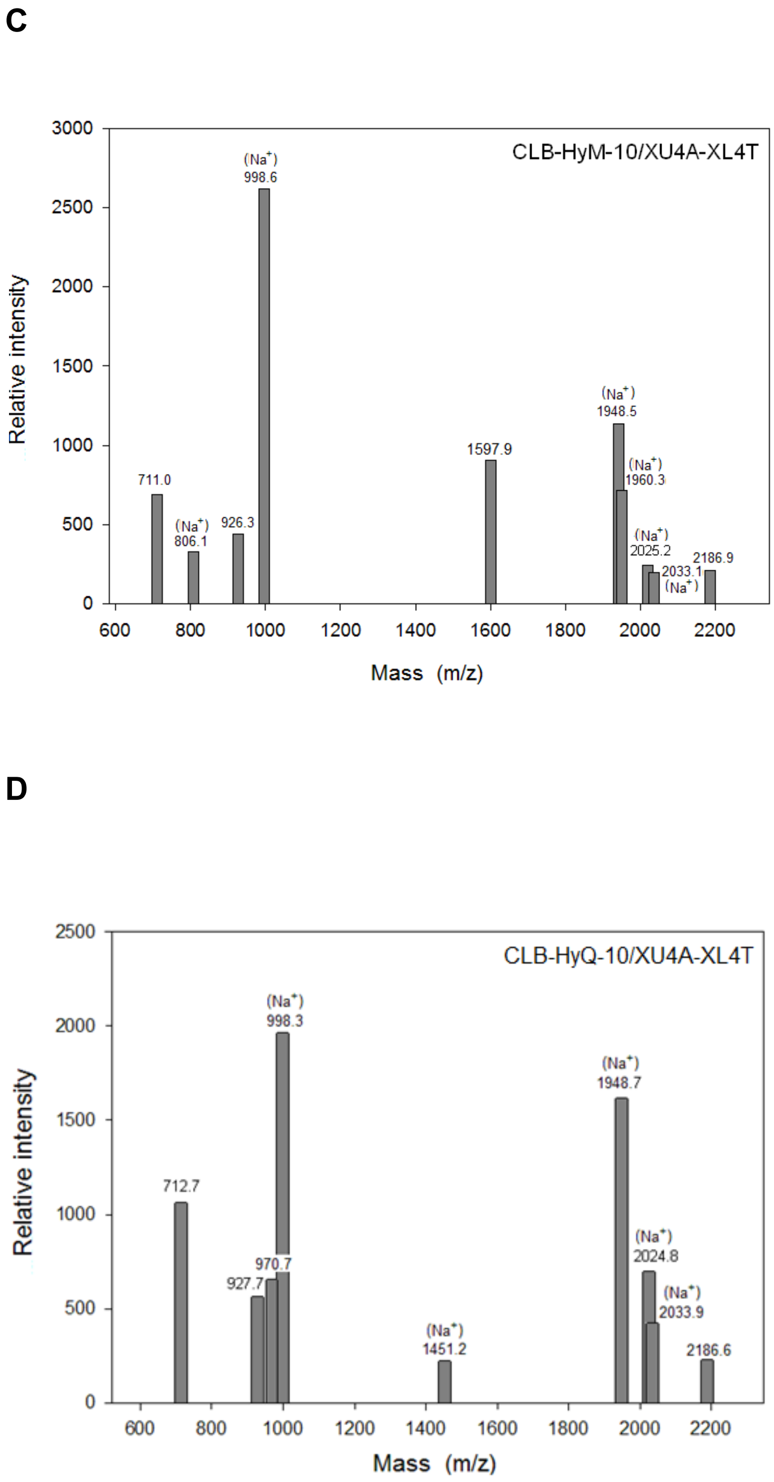
C
CLB-HyM-10/XU4A-XL4T
Relative intensity
3000
2500
2000
1500
1000
500
0
600
800
1000
1200
1400
1600
1800
2000
2200
Mass (m/z)
711.0
(Na$^+$) 806.1
926.3
(Na$^+$) 998.6
1597.9
(Na$^+$) 1948.5
(Na$^+$) 1960.3
(Na$^+$) 2025.2
2033.1 (Na$^+$)
2186.9
D
CLB-HyQ-10/XU4A-XL4T
Relative intensity
2500
2000
1500
1000
500
0
600
800
1000
1200
1400
1600
1800
2000
2200
Mass (m/z)
712.7
927.7
970.7
(Na$^+$) 998.3
(Na$^+$) 1451.2
(Na$^+$) 1948.7
(Na$^+$) 2024.8
(Na$^+$) 2033.9
2186.6

Figure [III]

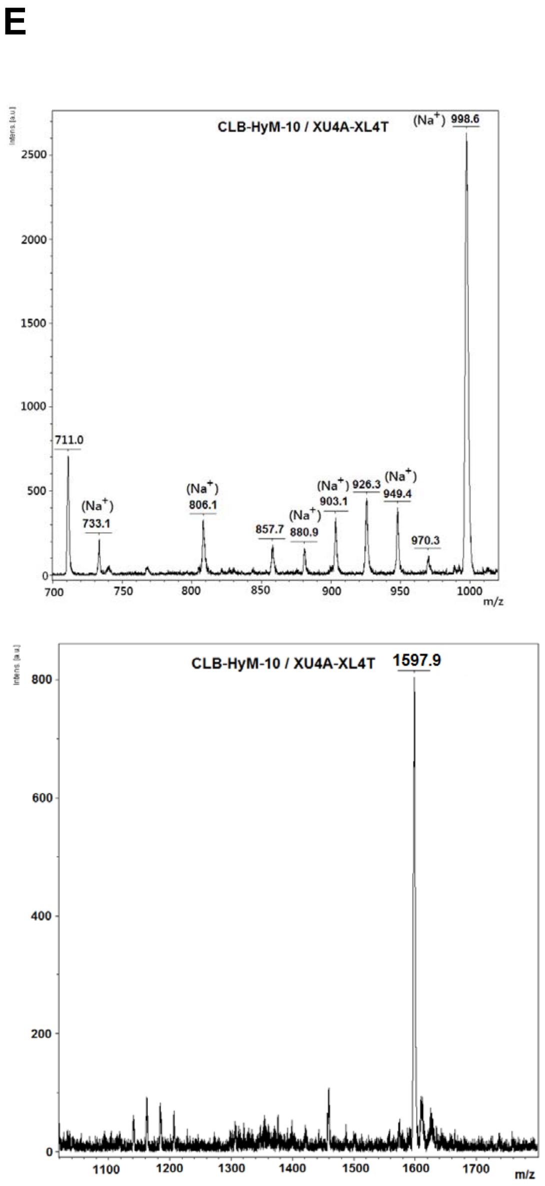
E
CLB-HyM-10 / XU4A-XL4T
Intens. [a.u.]
2500
2000
1500
1000
500
0
711.0
(Na+)
733.1
(Na+)
806.1
857.7
(Na+)
880.9
(Na+)
903.1
926.3
(Na+)
949.4
970.3
(Na+)
998.6
700
750
800
850
900
950
1000
m/z
CLB-HyM-10 / XU4A-XL4T
1597.9
Intens. [a.u.]
800
600
400
200
0
1100
1200
1300
1400
1500
1600
1700
m/z

Figure [III]

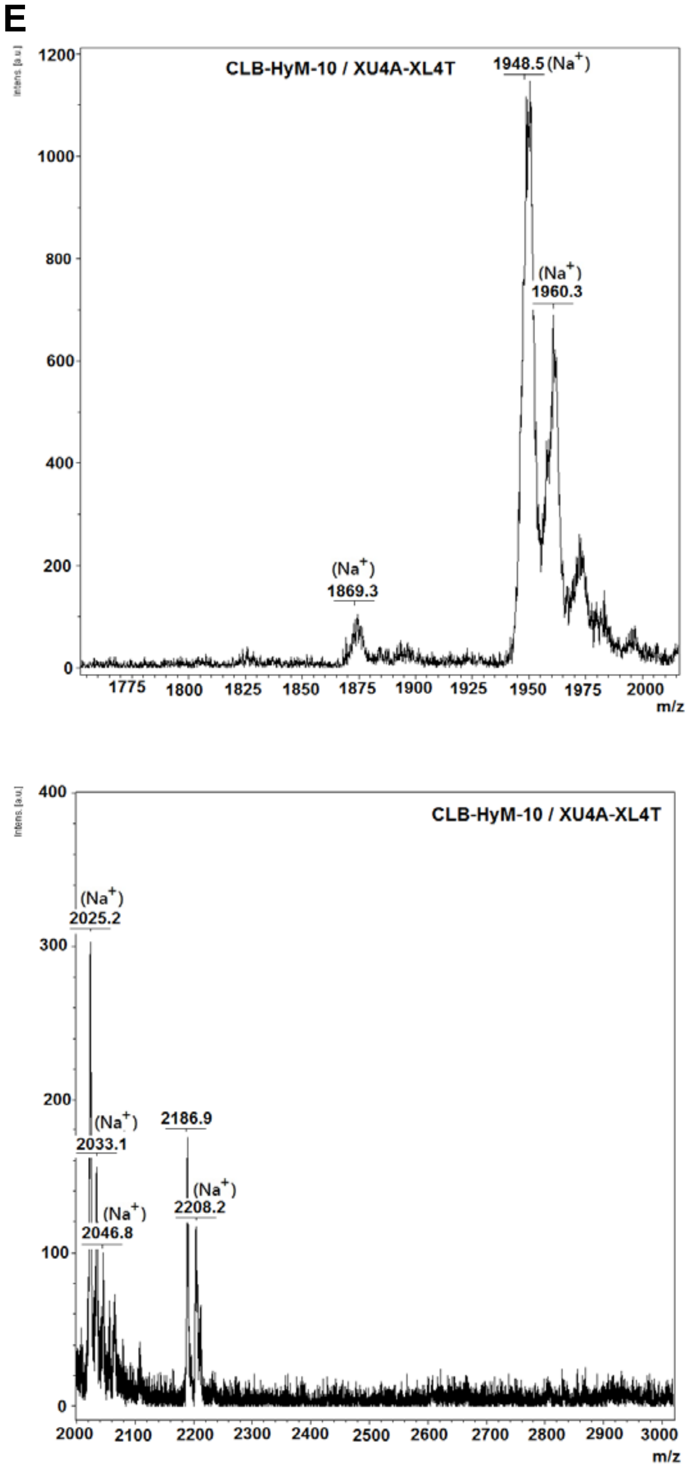
E
CLB-HyM-10 / XU4A-XL4T
Intens. [a.u.]
1200
1000
800
600
400
200
0
1948.5 (Na+)
(Na+)
1960.3
(Na+)
1869.3
1775
1800
1825
1850
1875
1900
1925
1950
1975
2000
m/z
CLB-HyM-10 / XU4A-XL4T
Intens. [a.u.]
400
300
200
100
0
(Na+)
2025.2
(Na+)
2033.1
(Na+)
2046.8
2186.9
(Na+)
2208.2
2000
2100
2200
2300
2400
2500
2600
2700
2800
2900
3000
m/z

Figure [III]

F

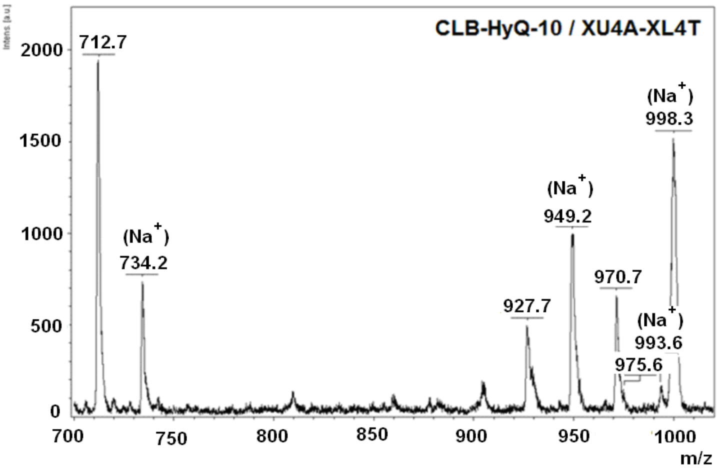

CLB-HyQ-10 / XU4A-XL4T
Intens. [a.u.]
2000
1500
1000
500
0
712.7
(Na+)
734.2
927.7
(Na+)
949.2
970.7
975.6
(Na+)
993.6
(Na+)
998.3
700
750
800
850
900
950
1000
m/z

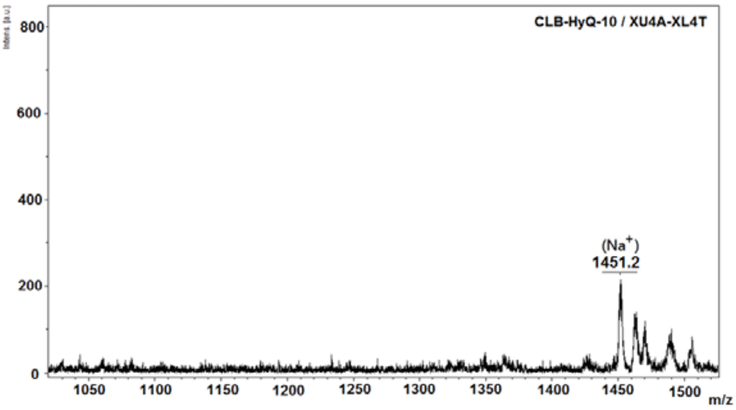

CLB-HyQ-10 / XU4A-XL4T
Intens. [a.u.]
800
600
400
200
0
(Na+)
1451.2
1050
1100
1150
1200
1250
1300
1350
1400
1450
1500
m/z

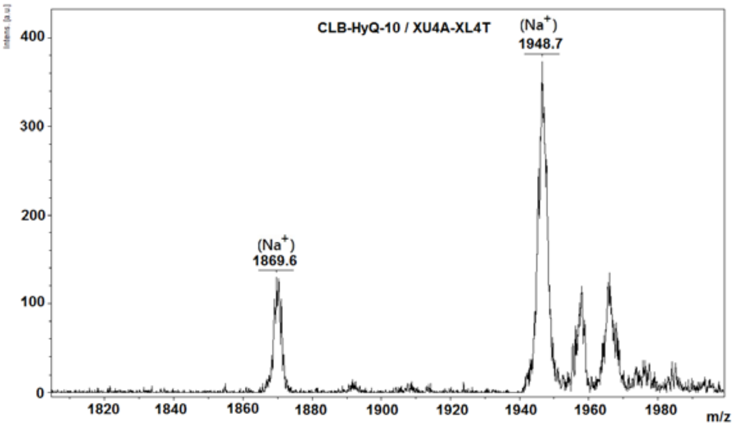

CLB-HyQ-10 / XU4A-XL4T
Intens. [a.u.]
400
300
200
100
0
(Na+)
1869.6
(Na+)
1948.7
1820
1840
1860
1880
1900
1920
1940
1960
1980
m/z

F

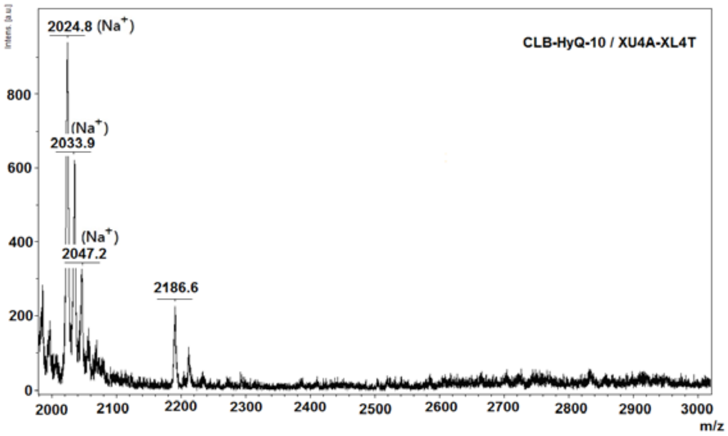
Intens [a.u.]
2024.8 (Na$^+$)
(Na$^+$)
2033.9
(Na$^+$)
2047.2
2186.6
CLB-HyQ-10 / XU4A-XL4T
0
200
400
600
800
2000
2100
2200
2300
2400
2500
2600
2700
2800
2900
3000
m/z

Figure [III]

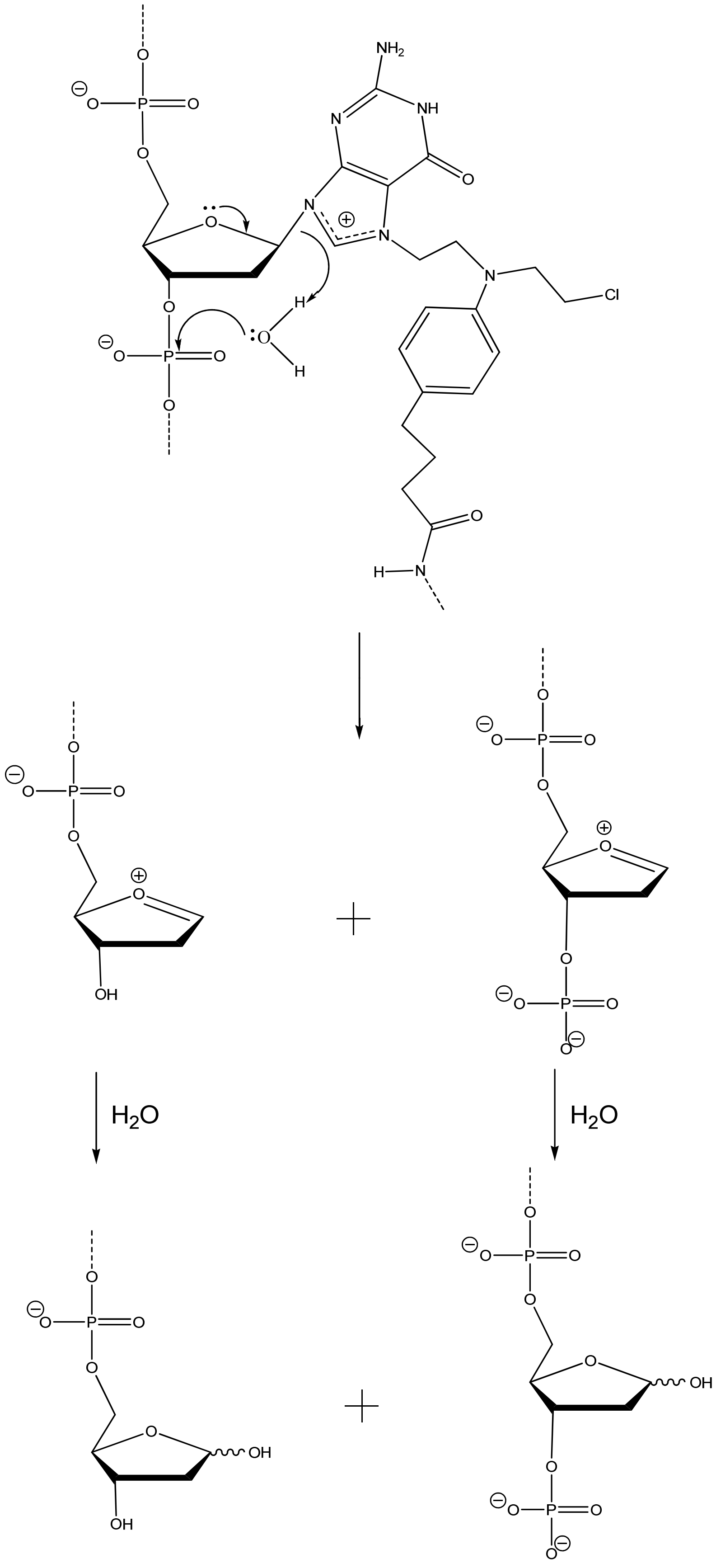

Figure [IV]

5’-A_1 - A_2 - G_3 - G_4 - A_5-G_6 -↓A_7↓-A_8-A_9 -A_{10}-T_{11}- A_{12}- 3’

H_2N-KR-$(Py)_4$-K-R-P_h-M- X X -M-P_h-R-K -$(Py)_4$-R-K-NH_2

3’-dr - C_{24}- C_{23}- T_{22}-C_{21}↓-T_{20}-T_{19}-T_{18}-T_{17}- A_{16}- T_{15}-5’

The chemical nuclease activity, energetics, and stepwise cleavage mechanism of chlorambucil-peptide conjugates are presented.